# Designing Poly[(*R*)-3-hydroxybutyrate]-Based Polyurethane Block Copolymers for Electrospun Nanofiber Scaffolds with Improved Mechanical Properties and Enhanced Mineralization Capability

**Kerh Li Liu,[†] Eugene Shi Guang Choo,[‡] Siew Yee Wong,[†] Xu Li,*[,†] Chao Bin He,[†] John Wang,[‡] and Jun Li*[,†,§]**

*Institute of Materials Research and Engineering, A*STAR (Agency for Science, Technology and Research), 3 Research Link, Singapore 117602, and Department of Materials Science and Engineering and Division of Bioengineering, Faculty of Engineering, National University of Singapore (NUS), 7 Engineering Drive 1, Singapore 117574*

*Received: March 1, 2010; Revised Manuscript Received: April 27, 2010*

Efforts to mineralize electrospun hydrophobic polyester scaffold often require prior surface modification such as plasma or alkaline treatment, which may affect the mechanical integrity of the resultant scaffold. Here through rational design we developed a series of polyurethane block copolymers containing poly[(*R*)-3-hydroxybutyrate] (PHB) as hard segment and poly(ethylene glycol) (PEG) as soft segment that could be easily fabricated into mineralizable electrospun scaffold without the need of additional surface treatment. To ensure that the block copolymers do not swell excessively in water, PEG content in the polymers was kept below 50 wt %. To obtain good dry and hydrated state mechanical properties with limited PEG, low-molecular-weight PHB-diol with $M_n$ 1230 and 1790 were used in various molar feed ratios. The macromolecular characteristics of the block copolymers were confirmed by $^1$H NMR spectroscopy, gel permeation chromatography (GPC), and thermal gravimetric analyses (TGA). With the incorporation of the hydrophilic PEG segments, the surface and bulk hydrophilicity of the block copolymers were significantly improved. Differential scanning calorimetry (DSC) revealed that the block copolymers had low PHB crystallinity and no PEG crystallinity. This was further confirmed by X-ray diffraction analyses (XRD) in both dry and hydrated states. With short PHB segments and soft PEG coupled together, the block copolymers were no longer brittle. Tensile measurements showed that the block copolymers with higher PEG content or shorter PHB segments were more ductile. Furthermore, their ductility was enhanced in hydrated states with one particular example showing increment in strain at break from 1090 to 1962%. The block copolymers were fabricated into an electrospun fibrous scaffold that was easily mineralized by simple incubation in simulated body fluid. The materials have good potential for bone regeneration application and may be extended to other applications by simply coating them with other biologically active substances.

## Introduction

In tissue engineering, a scaffold is used to support cell attachment, proliferation, differentiation, and tissue formation. The choice of materials and their processing into tissue engineering scaffold are of critical importance for successful application and are major areas of intense research.[1,2] It is not sufficient that the scaffold merely functions as a physical template for tissue formation, and many studies showed that the entire scaffold construct has to mimic the extracellular matrix (ECM) native to the cells and tissue of interest. This has generated much impetus to develop biomaterials with appropriate mechanical strength with specific surface chemistry that emulates natural ECM as well as to engineer a 3D structure with porosity that facilitates materials transport.[3−6]

In light of these, fibrous scaffolds obtained from electrospinning of biodegradable polymers have attracted widespread attention.[7,8] The appeal stems from their highly porous nature with well-defined nano- to microscale features that mimic natural ECM. Many biodegradable polyesters such as poly(lactide), poly(caprolactone), poly(glycolide), and poly(hydroxyalkanoates) (PHAs) have been used to this end.[9] However, their high hydrophobicity and lack of site for chemical modification often lead to poor scaffold−cell interaction and present a hurdle to incorporate biochemical molecules into the whole 3D construct.[10−12] Surface modifications like plasma or alkaline treatment of these scaffolds is an effective solution but might compromise the scaffold mechanical properties. Moreover, because the treatment is usually superficial, modification only occurred on the scaffold surface but not throughout the bulk.

Poly[(*R*)-3-hydroxybutyrate] (PHB) is a natural biopolyester found in many bacteria as energy source.[13] Its biocompatibility, biodegradability, and availability in very pure form free of catalyst contamination made it an attractive candidate for scaffold materials. However, because of its high hydrophobicity and crystallinity that is often detrimental for cell attachment as well as its brittleness that is resulted from the high crystallinity, widespread application of PHB as scaffold material is not seen. Among the many techniques used, the poor mechanical properties can be circumvented through physical blending of PHB with

* Corresponding authors. (X.L.) E-mail: x-li@imre.a-star.edu.sg. Tel: +65-6874-8421. Fax: +65-6872-7528. (J.L.) E-mail: bielj@nus.edu.sg. Tel: +65-6516-7273. Fax: +65-6872-3069.

[†] A*STAR (Agency for Science, Technology and Research).

[‡] Department of Materials Science and Engineering, Faculty of Engineering, National University of Singapore (NUS).

[§] Division of Bioengineering, Faculty of Engineering, National University of Singapore (NUS).

10.1021/jp1018247 
Published on Web 05/14/2010

compatible polymers that include poly(ethylene glycol) (PEG) and atactic-PHB.[14−16] Another strategy is through chemical modification of the PHB backbone by incorporating soft polymer segment such as PEG or other monomers such as hydroxyvalerate (HV), hydroxyhexanoate, and hydroxyoctanoate via biochemical route that can impart flexibility to or suppress crystallization of the PHB polymer backbone.[17−32] Recently, our laboratory demonstrated that PHB-based polyurethane block copolymers with highly ductile mechanical properties could be obtained through chain extension of hard PHB segments and soft PEG segments with hexamethylenediisocyanate (HDI).[20] We have also shown in another study that significant improvements in hydrated state mechanical properties of poly[(*R*)-3-hydroxybutyrate-*co*-(*R*)-3-hydroxyvalerate] (PHBV, 8 wt % HV content) matrix could be obtained by blending amphiphilic PHB-PEG alternating block copolymer into the PHBV matrix.[33]

Modification of PHB through the formation of polyurethane with PEG is of particular interest because the resultant block copolymers could have simultaneous improvements over their mechanical properties as well as hydrophilicity. Besides, as PHB crystallinity reduces with the presence of PEG, we could expect better cell attachment on PHB-PEG copolymers. With the aim to better mimic native ECM, the presence of hydrophilic PEG segment also presents an avenue to absorb or release bioactive agents into the entire scaffold materials, for instance, calcium phosphate minerals as in the case for bone regeneration.

In this article, we present a simple yet effective strategy to fabricate uniformly mineralizable scaffold from polyurethane block copolymers composed of PHB and PEG with good mechanical properties via electrospinning. We hereby synthesized a series of polyurethane block copolymers, termed as poly(PHB/PEG urethane)s, with good dry and hydrated state mechanical properties as well as enhanced mineralization capability based on PHB and PEG via chain extension using HDI for the following purposes. First, particular attention has been focused on the extent of PEG incorporation. It was capped at an optimum level to ensure good ductility on resultant copolymers in both dry and hydrated states, yet when electrospun into fibers, increment in hydrophilicity does not lead to overswelling of the polymeric fibers in aqueous environment. Second, variation in PHB content was achieved by changing molar feed ratios of low-molecular-weight PHB-diol rather than employing longer PHB-diol at constant feed ratio. The reason is to minimize PHB crystallization and improve the ductility of the block copolymers even at limited PEG content. Moreover, at similar copolymer molecular weight, the use of short PHB-diol over longer ones has the benefit of introducing more urethane bonds into each copolymer backbone. This in turn is advantageous for enhancement of mechanical properties of the final copolymer. The synthesized block copolymers were characterized using gel permeation chromatography (GPC), $^1$H NMR spectroscopy and thermal gravimetric analyses (TGA). Their crystallization behaviors and solid-state properties were also studied using differential scanning calorimetry (DSC) and wide-angle X-ray diffraction (XRD). The hydrophilicity and mechanical properties improvements in the block copolymers with respect to pristine PHB were ascertained with water uptake experiment and static water contact angle measurements as well as dry and hydrated state tensile strength measurements, respectively. To evaluate their suitability as scaffold material further, electrospun fibers were prepared from one of the copolymers and tested for its ability for calcium mineralization.

## Experimental Section

**Materials.** Natural source PHB and PHBV with hydroxyvalerate (HV) content of 8 wt % were purchased from Aldrich. Both purified PHB and PHBV were obtained by first dissolving the as received material in chloroform, followed by filtration and precipitation of the soluble fraction into *n*-hexane. PEG with $M_n$ ca. 2000 was purchased from Aldrich and was purified by precipitating its 1,2-dichloroethane solution into anhydrous diethyl ether and vacuum-dried before use. Its $M_n$ and polydispersity index (PDI) were found to be 2000 and 1.03, respectively. Bis(2-methoxyethyl) ether (diglyme; 99%), ethylene glycol (99%), dibutyltin dilaurate (95%), hexamethylene diisocyanate (HDI) (98%), methanol, diethyl ether, and 1,2-dichloroethane (99.8%) were purchased from Aldrich. 1,2-Dichloroethane was dried by distilling over $CaH_2$ prior to use.

Low-molecular-weight PHB-diols were obtained from transesterification of natural source PHB and ethylene glycol with the aid of catalyst dibutyltin dilaurate in diglyme at 140 °C, as previously reported.[34] Small aliquots of reaction mixture were sampled periodically to monitor the reduction in polymer molecular weight. Upon reaching a desired molecular weight, the reaction was stopped by precipitating the mixture into cold water. From GPC, the $M_n$ and PDI of the PHB-diols were found to be 1230 and 1.24 and 1790 and 1.22, respectively.

**Synthesis of Poly(PHB/PEG urethane)s.** Random multiblock poly(PHB/PEG urethane)s were synthesized through coupling of PHB-diol and PEG with HDI in 1,2-dichloroethane at 75 °C in the presence of catalyst dibutyltin dilaurate. The amount of HDI added corresponded to an equimolar ratio of isocyanate groups to total hydroxyl groups present. The synthetic strategy is a modification from our previous method,[20] whereby different prepolymer molar ratios were used instead of fixing them at a one-to-one ratio. Typically, 623 mg of PHB-diol ($M_n$ 1790, 0.348 mmol) and 174 mg of PEG ($M_n$ 2000, 0.087 mmol) were weighed in a two-necked 250 mL round-bottomed flask and dried at 95 °C under high vacuum for at least 15 h. Then, an excess (20 mL) of anhydrous 1,2-dichloroethane was added to the reaction flask under dry nitrogen atmosphere, and any trace water in the system was removed through azeotropic distillation. The reaction flask was then cooled to 75 °C with ~3 mL of solvent left in it. HDI (73 mg, 0.435 mmol) was then added into the reaction mixture followed by two drops (~8 mg) of dibutyltin dilaurate catalyst. The reaction proceeded at a constant temperature of 75 °C under dry nitrogen atmosphere with continuous stirring for 48 h. The reaction product was then precipitated into a mixture of anhydrous diethyl ether and methanol (95/5, v/v) to remove any unreacted precursors and catalyst. The product was further purified by redissolving it in chloroform followed by precipitation in diethyl ether. Yield: 0.57 g (71.6%). GPC (THF): $M_n$ = 24 300, PDI = 1.67. $^1$H NMR (400 MHz, $CDCl_3$, $\delta$): 1.26 (d, $-OCH(C\underline{H}_3)CH_2CO_2-$), 1.32 (br, $-OCONHCH_2CH_2C\underline{H}_2C\underline{H}_2CH_2CH_2NHCO_2-$), 1.48 (br, $-OCONHCH_2C\underline{H}_2CH_2CH_2C\underline{H}_2CH_2NHCO_2-$), 2.44−2.63 (m, $-OCH(CH_3)C\underline{H}_2CO_2-$), 3.13 (t, $-OCONHC\underline{H}_2CH_2CH_2CH_2CH_2C\underline{H}_2NHCO_2-$), 3.64 (s, $-OC\underline{H}_2C\underline{H}_2O-$ of PEG block), 4.21 (t, $-OCH_2C\underline{H}_2OCO-$ of PEG next to urethane group), 4.25 (s, $-CO_2C\underline{H}_2C\underline{H}_2OCO-$ of PHB next to urethane group), 5.21−5.29 (m, $-OC\underline{H}(CH_3)CH_2CO_2-$).

**Molecular Characterizations.** GPC analyses were carried out with a Shimadzu SCL-10A and LC-8A system equipped with two Phenogel 5 $\mu$ 50 and 1000 Å columns (size: 300 × 4.6 mm) coupled in series and a Shimadzu RID-10A refractive index detector. THF was used as the mobile phase at a flow rate of 0.20 mL/min at 45 °C. Monodispersed PEG standards

were used to calibrate the system. $^1$H NMR spectra were recorded on a Bruker AV-400 NMR spectrometer at 400 MHz at room temperature, and chemical shifts were reported in ppm with reference to chloroform solvent peak ($\delta$ 7.26).

**Thermal Analysis.** DSC measurements were performed on a TA Instruments 2920 differential scanning calorimeter equipped with an autocool accessory and calibrated using indium. The following protocol was used for each sample: heating from room temperature to 180 at 5 °C min$^{-1}$, holding at 180 °C for 2 min, cooling from 180 to −30 at 5 °C min$^{-1}$, holding at −30 °C for 2 min, and finally reheating from −30 to 180 at 5 °C min$^{-1}$. Data collected on the first cooling and second heating runs were analyzed, and peak maxima were taken as transition temperatures. Thermogravimetric analyses (TGA) were carried out on a TA Instruments SDT 2960. Samples were heated at 20 °C min$^{-1}$ from room temperature to 800 °C under a dynamic nitrogen atmosphere (flow rate = 70 mL min$^{-1}$).

**Wide-Angle X-ray Diffraction (XRD).** XRD measurements were carried out on a Bruker GADDS diffractometer with an area detector operating under Cu Kα (1.5418 Å) radiation (40 kV, 40 mA) at room temperature. Film or powder samples were mounted on sample holder with double-sided adhesive tape.

**Static Water Contact Angle Measurement.** Poly(PHB/PEG urethane) thin films were prepared from their 1,2-dichloroethane solution (10 mg mL$^{-1}$) through spin-coating onto precleaned glass slides. Static water contact angles of the films were measured by the sessile method at room temperature under an air atmosphere using an NRL-100-0-(230) contact angle goniometer (Ramè-Hart, New Jersey). The droplet volume used for measurement was 2 μL. Telescope with a magnification power of ×23 was equipped with a protractor of 0.1° graduation. Each contact angle reported was averaged from at least 10 readings from different parts of the film surface and is reliable to 2°.

**Water Uptake Measurement.** Poly(PHB/PEG urethane) films were prepared by casting a 10 mL polymer solution (30 mg mL$^{-1}$) using 1,2-dichloroethane as solvent onto a 6 cm diameter PTFE dish. Following slow evaporation of 1,2-dichloroethane, the films were dried under high vacuum at 50 °C for 2 days to remove trace solvent. The dried films were then cut into discs (8 mm diameter, 80−110 μm thickness) and immersed in deionized water at 37 °C to simulate body temperature. At predetermined time intervals, the hydrated polymer discs were removed from the water, and the surface water was blotted up lightly using Kimwipes. The total cumulative time for measurement of water uptake was 3 h for each disk. The amount of water absorbed by the polymer discs was determined by measuring the weight difference of the discs before and after swelling. The percentage of water uptake was calculated using the following equation

$$\text{water uptake (\%)} = 100 \times (W_w - W_d)/W_d$$

where $W_d$ and $W_w$ are the weight of sample film in dry and hydrated states, respectively. The reported values for each sample were averaged from five replicates.

**Tensile Strength Measurement.** Films, prepared similarly as above, were cut into 20 × 6 mm$^2$ rectangles with thickness of 80−110 μm. The thickness of the films was measured using a micrometer. The tensile strength measurements were then performed using an Instron 5543 microforce tester with a deformation rate of 40 mm min$^{-1}$ and a free length of 10 mm. For hydrated state measurements, the samples were immersed in phosphate buffered saline for 24 h at 37 °C and then taken out, blotted dry with Kimwipes paper, and had their thickness measured using a micrometer immediately before their tensile strength measurements. An average of five measurements was reported as the mean ± standard deviation for each sample.

**Electrospinning of Poly(PHB/PEG urethane) and PHBV Fibers.** Poly(PHB/PEG urethane) solution for electrospinning was prepared by dissolving the purified polymer in a mixed solvent of chloroform and 1,2-dichloroethane (2/3; W/W) at 9 wt %. The mixture was stirred at 50 °C overnight to ensure complete dissolution of polymer. Electrospinning was carried out with the prepared poly(PHB/PEG urethane) solution at an applied voltage of 12 kV using 22 gauge size needle (inner diameter of opening is ∼0.4 mm) with a needle-to-collector distance of 150 mm. The flow rate of the polymer solution was set at 0.5 mL h$^{-1}$ using a syringe pump. For this study, a stationery flat aluminum foil was used to collect electrospun poly(PHB/PEG urethane) fibers. Electrospun PHBV fiber was fabricated in the same manner as a control for mineralization study.

**Characterization of Electrospun Fibers.** The morphology of electrospun poly(PHB/PEG urethane) fibers was examined using a field emission scanning electron microscope (SEM, JEOL JSM-6700F). Fiber diameter has been measured using software ImageJ and reported as the mean ± standard deviation ($n$ = 20).

**Mineralization of Electrospun Fibers.** Small pieces of the electrospun PHBV or PH2E2(4:1) fiber mats were immersed in ×2.5 or ×10 simulated body fluid (SBF) over 12 h for mineralization to take place. The mineralized fibers were then cleaned with deionized water and freeze-dried before subjected to SEM (JEOL JSM-5600) investigation. SBF (×10) was prepared according to literature recipe with the following composition in g L$^{-1}$: NaCl (58.43), KCl (0.37), $CaCl_2 \cdot H_2O$ (3.68), $MgCl_2 \cdot 6H_2O$ (1.02), $Na_2HPO_4$ (1.42), $NaHCO_3$ (0.84).[35] SBF (×2.5) was obtained by diluting the more concentrated SBF. Minerals content on each of the mineralized fiber mat was estimated using TGA by heating the mineralized sample to 800 °C under a $N_2$ atmosphere. Because poly(PHB/PEG urethane)s are completely degraded at ∼450 °C, any residue left will come from the deposited minerals, and this serves as a basis for the quantification of minerals content in the mineralized fiber mat. However, because pure minerals that were precipitated from SBF in the absence of fiber mat also experienced weight loss when heated to 800 °C, leaving behind 78 wt % of residue, the amount of residue from all mineralized samples must be corrected accordingly to obtain the actual minerals content. The correction is reflected by the following equation

$$\text{mineral content on mineralized fiber mat (wt \%)} = 100 \times \text{fiber mat residue (wt \%)}/\text{pure minerals residue (wt \%)}$$

## Results and Discussion

**Synthesis and Molecular Characterizations of Poly(PHB/PEG urethane)s.** Poly(PHB/PEG urethane)s described here were obtained through isocyanate coupling of PHB-diol and PEG precursors, as previously reported[20] and depicted here in Scheme 1. However, in contrast with the previous report, PHB content of the series of block copolymers are tuned by adjusting the molar feed ratio of PHB-diol and PEG while keeping the molecular weight of PHB-diol unchanged. This approach allows us to limit PEG content in the block copolymer between 30 to 50 wt % with the use of low-molecular-weight PHB-diol. The rationale behind such block copolymer design is two-fold. First,

**SCHEME 1: Synthetic Route of Poly(PHB/PEG urethane)s from High Molecular Weight PHB and PEG**

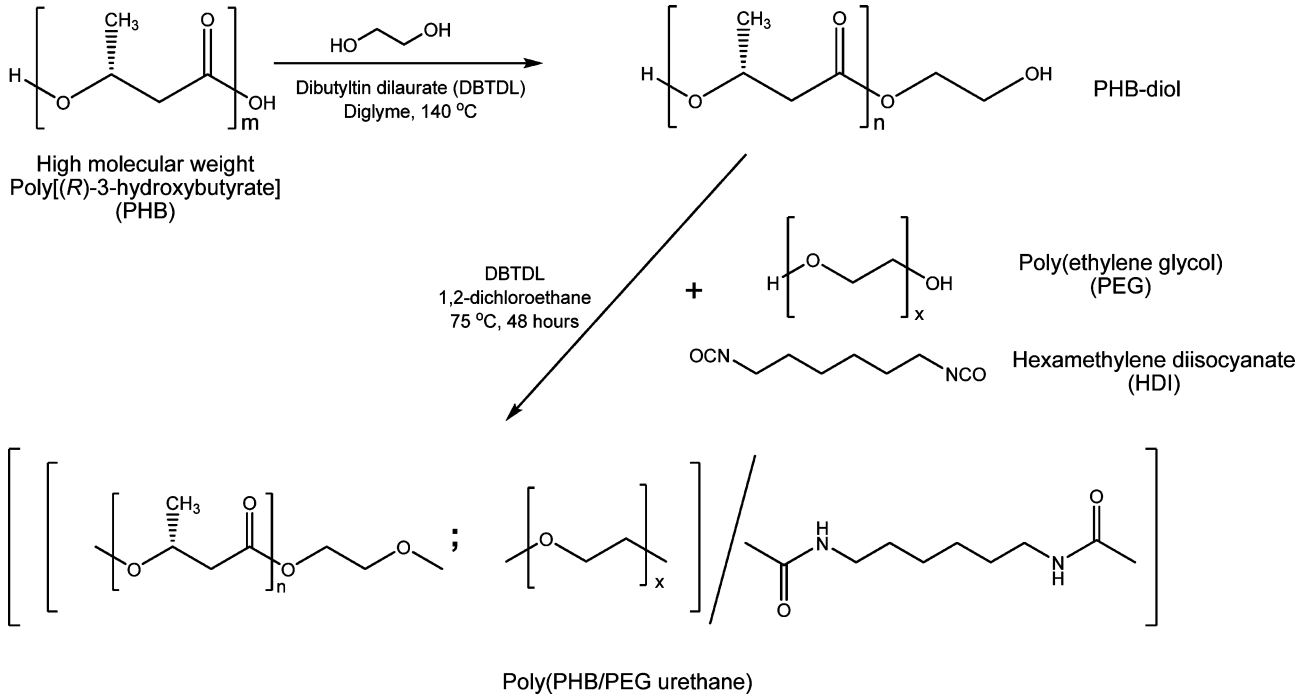


**TABLE 1: Molecular Characteristics of Poly(PHB/PEG urethane)s**

| poly(PHB/PEG urethane)s[a] | $M_n$ of PHB-diol used[b] | molar feed ratio of PHB-diol to PEG | $M_n$ ( $\times 10^3$)[b] | PDI[b] | PHB content (wt %) theoretical[c] | NMR[d] | TGA[e] | yield (%) |
|---|---|---|---|---|---|---|---|---|
| PH1E2(2.5:1) | 1230 | 2.5:1 | 22.7 | 1.70 | 54.3 | 49.7 | 55.7 | 55.2 |
| PH1E2(5:1) | 1230 | 5:1 | 40.0 | 1.74 | 67.1 | 65.9 | 67.2 | 53.0 |
| PH2E2(2:1) | 1790 | 2:1 | 23.9 | 1.59 | 58.8 | 54.9 | 55.9 | 60.3 |
| PH2E2(4:1) | 1790 | 4:1 | 24.3 | 1.67 | 71.6 | 67.8 | 69.6 | 71.6 |

[a] Poly(PHB/PEG urethane)s are denoted PH*p*E*q*(*a*:*b*), where *p* and *q* represent the indicative molecular weight of PHB-diol and PEG in kilograms per mole, respectively, whereas *a*:*b* depicts the molar feed ratio of PHB-diol to PEG. [b] Determined by GPC. [c] Calculated based on the molar feed ratio of PHB-diol, PEG, and HDI. [d] Calculated from $^1$H NMR results. [e] Calculated from thermogravimetric analyses.

because the polymers are intended for application as electrospun fibrous scaffold, limiting their PEG content would prevent excessive swelling that affects the dimensional stability of the fibrous construct under physiological environment, in addition to imparting optimal dry and hydrated state mechanical properties to the block copolymer. Second, because of the limited amount of PEG we could use, brittleness of the block copolymer must be further overcome by an inherent lower crystallizability of its PHB segment, which comes best with short PHB segment. Here four poly(PHB/PEG urethane)s with PHB contents ranging from 50 to 70 wt % were synthesized from a PEG with $M_n$ of 2000 and two PHB-diols with $M_n$ of 1230 and 1790, respectively, at different molar feed ratios. The ratios are given in Table 1, along with reaction yields as well as molecular weight information and respective PHB contents for each polyurethane synthesized. The poly(PHB/PEG urethane)s are named as PH*p*E*q*(*a*:*b*), where *p* and *q* each represent the indicative molecular weight of PHB and PEG precursors used, respectively, in kilograms per mole, whereas *a*:*b* depicts the molar feed ratio of PHB-diol to PEG.

The successful syntheses of the poly(PHB/PEG urethane)s are first evidenced by the presence of unimodal GPC elution peak occurring at a higher molecular weight region than those of both PHB-diol and PEG precursors. As an example, the GPC trace of PH2E2(4:1) is shown in the inset of Figure 1 along with its precursors. The clean chromatogram also implies that the obtained block copolymer is free from unreacted prepolymers. With the moderate-to-good block copolymerization yields in mind, the unimodal molecular weight distribution also testifies the efficient coupling of PHB-diol with PEG using HDI and effective purification through simple polymer precipitation. The molecular weights of the obtained poly(PHB/PEG urethane)s are between $2.0 \times 10^4$ and $4.0 \times 10^4$ with relatively narrow polydispersity indices ranging from 1.59 to 1.74.

The formation of block copolymers with PHB and PEG segments is also confirmed by $^1$H NMR spectroscopy. As shown in a typical $^1$H NMR spectrum (Figure 1), the methine, methylene, and methyl protons of PHB segment can be seen at around $\delta$ 5.3, 2.5, and 1.3, respectively, whereas PEG methylene protons can be found at $\delta$ 3.6. In addition, $^1$H NMR peaks with lower intensities at $\delta$ 4.3, 4.2, 3.1, 1.5, and 1.3 can be assigned to PHB-diol and PEG protons adjacent to urethane functionalities as well as three sets of methylene protons originated from HDI, respectively. Together with GPC data, they strongly justify the formation of poly(PHB/PEG urethane)s.

Moreover, a quantitative analysis on the intensity ratio of PHB methine proton peak at $\delta$ 5.3 and PEG methylene proton peak at $\delta$ 3.6 provides estimation on PHB or PEG content in the block copolymer. The calculated PHB contents for the entire series of block copolymers range between 50 and 70 wt % and are listed in Table 1, along with similar estimations obtained from thermogravimetric analyses. The calculations of PHB

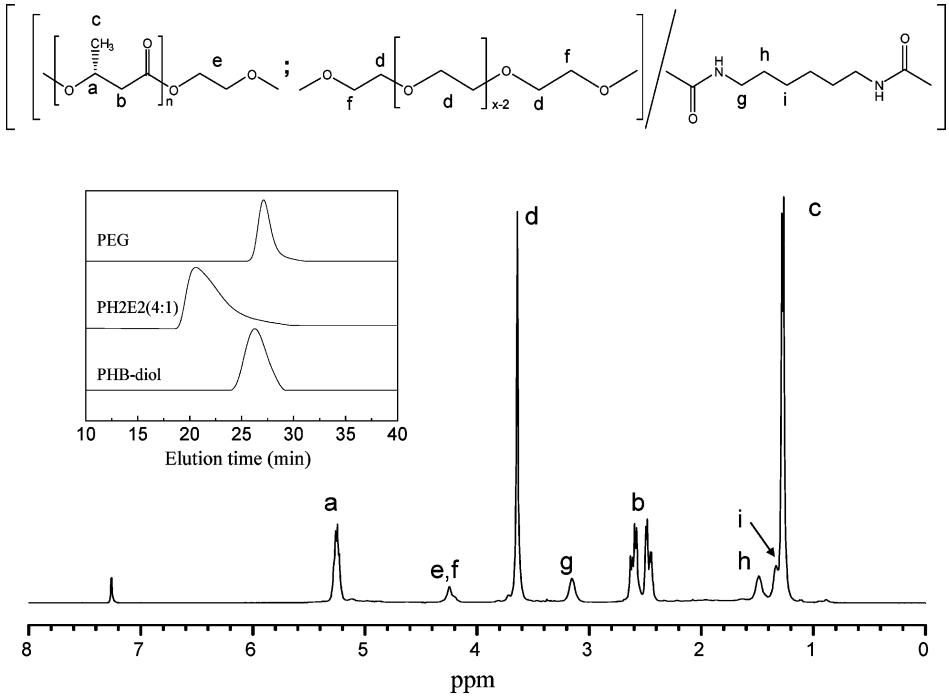


**Figure 1.** $^1$H NMR spectrum of PH2E2(4:1) with corresponding peak assignments. Inset: GPC chromatogram of PH2E2(4:1) along with its PEG ($M_n$ 2000) and PHB ($M_n$ 1790) precursors.

**TABLE 2: Crystallization, Cold Crystallization, and Melting Temperatures for PEG, PHB-diol, and PHB Segment of Poly(PHB/PEG urethane)s along with the Corresponding Enthalpy Changes and Degree of Crystallinity[a]**

| poly(PHB/PEG urethane)s[b] | $T_c$ (°C)[c] | $\Delta H_c$ (J g$^{-1}$)[c] | $T_{cc}$ (°C)[d] | $\Delta H_{cc}$ (J g$^{-1}$)[d] | $T_m$ (°C)[e] | $\Delta H_m$ (J g$^{-1}$)[e] | $X_c$ (%)[f] |
|---|---|---|---|---|---|---|---|
| PEG ($M_n$ 2000) | 33.9 | 160.1 | | | 55.5 | 164.3 | 80.2 |
| PH1E2(2.5:1) | | | 30.5 | 30.2 | 114.6 | 49.8 | 34.0 |
| PH1E2(5:1) | 68.1 | 52.7 | | | 137.7 | 58.7 | 40.0 |
| PH2E2(2:1) | 32.5 | 28.9 | | | 128.1 | 46.9 | 32.0 |
| PH2E2(4:1) | 39.7 | 42.8 | | | 130.0 | 53.4 | 36.4 |
| PHB-diol ($M_n$ 1230) | 89.3 | 85.4 | | | 151.3 | 103.3 | 70.5 |
| PHB-diol ($M_n$ 1790) | 67.1 | 79.9 | | | 144.8 | 98.4 | 67.1 |

[a] Enthalpy changes were calculated based on the formula $\Delta H = \Delta H_i/W_i$, where $\Delta H_i$ is the area of the exothermic or endothermic peak for PEG or PHB read from DSC thermograms, and $W_i$ is the weight fraction of PEG or PHB segment. [b] Poly(PHB/PEG urethane)s are denoted PH*p*E*q*(*a*:*b*), where *p* and *q* represent the indicative molecular weight of PHB-diol and PEG in kilograms per mole, respectively, whereas *a*:*b* depicts the molar feed ratio of PHB-diol to PEG. [c] Crystallization temperatures of PEG or PHB and corresponding enthalpy changes determined in DSC first cooling run. [d] Cold crystallization temperatures of PHB and corresponding enthalpy changes determined in DSC second heating run. [e] Melting temperatures of PEG or PHB and corresponding enthalpy changes determined in DSC second heating run. [f] PEG or PHB crystallinity calculated from melting enthalpy changes. Reference value of 205.0 and 146.6 J g$^{-1}$ for completely crystallized PEG and PHB, respectively, were used.[28]

content from thermogravimetric analyses are based on weight-loss analyses of the block copolymers when they were thermally degraded under inert atmosphere. The block copolymers demonstrated stepwise degradation profile that started with PHB segment, followed by HDI linker and completed with PEG segment, as shown in Figure S1 of the Supporting Information. PHB content in each polymer is then obtained from the percentage of weight loss at the end of PHB degradation. It can be seen from Table 1 that results from both $^1$H NMR spectroscopy and thermogravimetric analyses are very close to each other. More importantly, they corroborate well with theoretical values based on precursors and HDI feed ratios. This shows that the composition of the final block copolymer can be well controlled through the selection of precursor with suitable length and careful tuning of reactants feed ratios.

**Crystallization Behavior and Solid State Properties of Poly(PHB/PEG urethane)s.** To probe the crystallization behavior of the obtained poly(PHB/PEG urethane)s, DSC was used to detect any melting or crystallization transitions and measure the amount of heat flow involved. The DSC results are tabulated in Table 2. As shown in Figure 2, the PEG precursor melted at a characteristic temperature of ~56 °C with a sharp endothermic peak in the second heating run, whereas the two PHB-diols melted at 145 to 151 °C with multiple transitions as a result of recrystallization during the heating process.[36] For all of the poly(PHB/PEG urethane)s, only melting endotherms near the melting temperature of PHB precursor are observed. This suggests that only PHB segments in the block copolymers are able to form crystalline phase, whereas PEG segments remain amorphous. The degrees of PHB crystallinity of all the block copolymers were calculated from the melting enthalpy changes measured in the second heating runs and listed in Table 2. The degrees of PHB crystallinity in all of the poly(PHB/PEG urethane)s varied from 32 to 40% and are much lower than those of the PHB-diols used, which are around 67 to 71%. The significant reduction in PHB crystallinity can thus be attributed to the amorphous PEG present. The origin for such reduction in PHB crystallinity can be traced to the disruption PHB chain packing by PEG segments that are covalently coupled to PHB during crystallization. Similarly, the complete lack of PEG

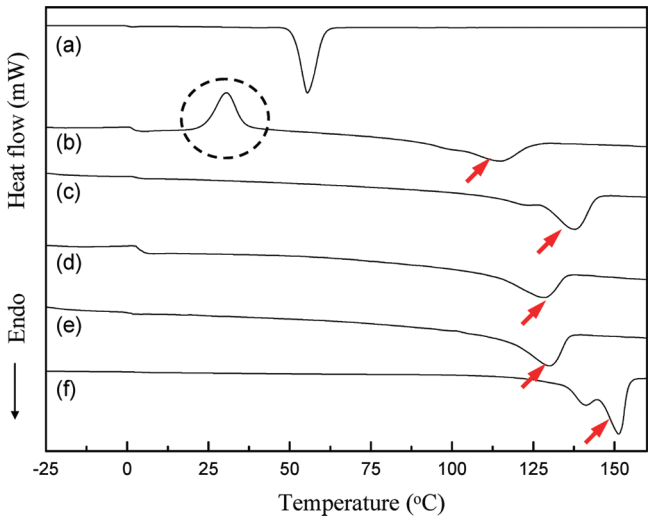


**Figure 2.** DSC second heating curves of (a) PEG ($M_n$ 2000), (b) PH1E2(2.5:1), (c) PH1E2(5:1), (d) PH2E2(2:1), (e) PH2E2(4:1), and (f) PHB-diol ($M_n$ 1230). Melting endotherms of PHB segment on all polymers are marked with arrows. The dotted circle highlights cold crystallization exotherm of PHB segment in PH1E2(2.5:1).

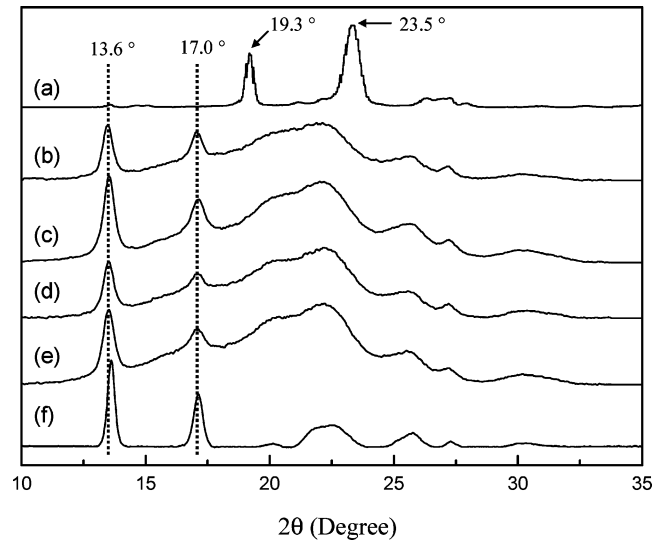


**Figure 3.** XRD results of PHB-diol, PEG, and poly(PHB/PEG urethane) films in dry state: (a) PEG ($M_n$ 2000), (b) PH1E2(2.5:1), (c) PH1E2(5:1), (d) PH2E2(2:1), (e) PH2E2(4:1), and (f) PHB-diol ($M_n$ 1790). Diffraction peaks of crystalline PHB are marked with dotted lines.

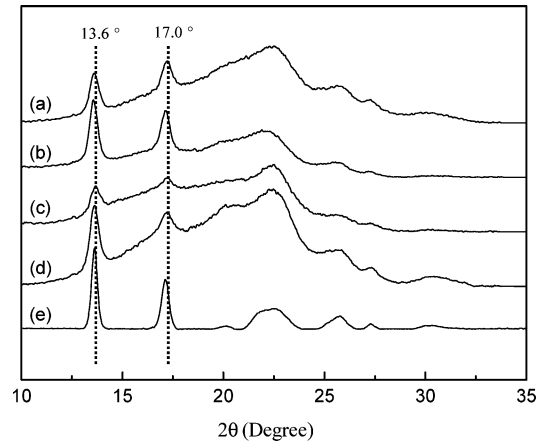


**Figure 4.** XRD results of PHB-diol in dry state and hydrated poly(PHB/PEG urethane) films after soaking in water at 37 °C for 24 h: (a)PH1E2(2.5:1), (b) PH1E2(5:1), (c) PH2E2(2:1), (d) PH2E2(4:1), and (e) PHB-diol ($M_n$ 1790). Diffraction peaks of crystalline PHB are marked with dotted lines.

crystallinity in all of the block copolymer samples can be ascribed to the mutual interference from PHB segments present.

The effectiveness of using short PHB segments in reducing PHB crystallinity is evident when we compare the PHB crystallinities of PH1E2(2.5:1) and PH2E2(2:1) with another poly(PHB/PEG urethane) synthesized from longer PHB-diol with $M_n$ of 3200 but slightly lower PHB content, PHE(32−33) found in our previous report.[20] The PHB crystallinities of PH1E2(2.5:1) and PH2E2(2:1) are 34 and 32%, respectively; whereas at a slightly lower PHB content of 46%, PHE(32−33) had a much higher PHB crystallinity of 45%. Moreover, in contrast with PH2E2(2:1), which contains similar PHB content but longer PHB segment, PHB crystallization in PH1E2(2.5:1) is totally prevented during the first cooling run (Figure S2 in Supporting Information) and is only feasible on subsequent heating, as reflected by the presence of cold crystallization transition in Figure 2b. This shows that the shorter PHB segment does encounter greater difficulty to crystallize. The phenomenon is presumably due to a higher density of urethane bonds, which could retard the crystallization of PHB segments.

To verify the presence of PHB crystalline phase in the block copolymers, wide-angle X-ray diffraction studies were carried out. As shown in Figure 3, two intense diffraction peaks are observed at 13.6 and 17.0°. They are the characteristic diffraction peaks of (020) and (110) planes of α-helical PHB crystalline phase,[37] respectively, and hence signify the presence of PHB crystalline phase in all of the block copolymers and PHB-diol. PEG crystalline diffraction peaks that are expected at 19.3 and 23.5° are absent in the block copolymer samples. The observations confirm that the semicrystalline nature of the block copolymers is brought about solely by PHB segments. The PHB crystalline phase can still be clearly observed in hydrated samples, as shown in Figure 4, with some reduction in peak intensity with reference to amorphous background, especially in PH1E2(2.5:1) and PH2E2(2:1) where more PEG is present. As PEG is water absorbing and with the fact that some PEG segments are trapped in PHB crystalline lamellae, immersing the block copolymer films into water will cause water diffusing into the whole polymer films, including PHB crystalline phase. This explains the relative reduction of PHB crystallinity in hydrated films as compared with dry ones, and such understanding will help us comprehend the changes in mechanical properties of the block copolymer between dry and hydrated states, which will be discussed later.

**Hydrophilicity.** The hydrophilicity of the block copolymers was characterized through static water contact angle measurements and by measuring their propensity to absorb water in terms of percentage water uptake. The latter examines bulk hydrophilicity, whereas the previous gives an idea on surface hydrophilicity. In the static water contact angle measurements, hydrophobic natural source PHB demonstrates the highest contact angle at ∼75°. As presented in Figure 5, the water contact angles then reduce in the order of PH2E2(4:1) > PH1E2(5:1) ≈ PH2E2(2:1) > PH1E2(2.5:1) to ∼65°. The decreasing trend that implies increased surface hydrophilicity, albeit marginal, is proportional to the PEG content within the block copolymers. In the water uptake experiment, all of the poly(PHB/PEG urethane) films typically reach equilibrium water uptake in 10 to 20 min of water immersion. (See Figure S3 in the Supporting Information.) As illustrated in Figure 6, whereas pristine PHB absorbs water only around 5% of its weight

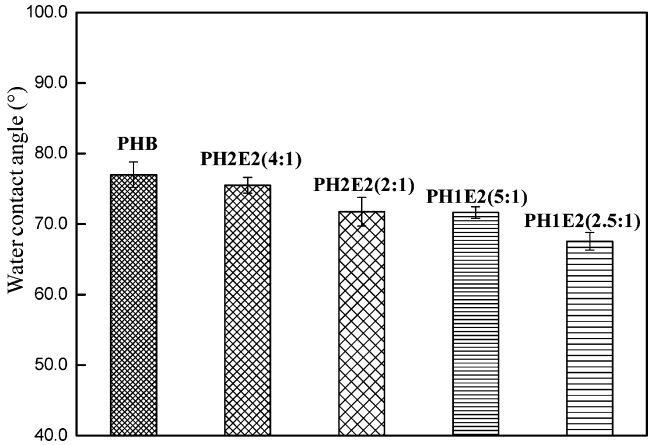


**Figure 5.** Static water contact angles of natural source PHB and poly(PHB/PEG urethane)s with identical PEG segment length ($M_n$ = 2000). The reported value for each sample was obtained from 10 measurements.

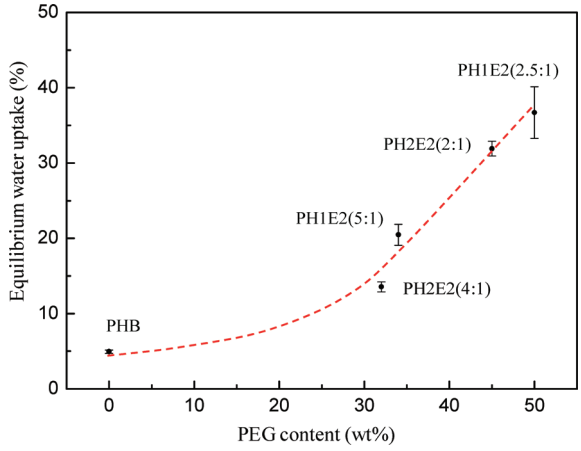


**Figure 6.** Equilibrium water uptake of poly(PHB/PEG urethane) films as a function of PEG content calculated from $^1$H NMR spectra. The reported value for each sample was obtained from five replicates.

because of its high hydrophobicity, the incorporation of PEG drastically increases the equilibrium water uptake in the block copolymers. With an increase in PEG content from 32 to 50 wt %, the amount of water absorbed increases from 14 to 36%. The moderate improvement in bulk hydrophilicity of these block copolymers over pristine PHB is critical for their application as scaffold materials. First, this improves cell−scaffold interaction. Second, the moderate increment in hydrophilicity prevents overswelling of scaffold in aqueous media, which may compromise dimensional stability of scaffold. For instance, with only light swelling in water, PH2E2(4:1) electrospun fibrous scaffold is able to retain its fibrous morphology after 4 days of immersion in culture media while supporting healthy cell proliferation. (See Figure S4 in Supporting Information.) Finally, the increased hydrophilicity also enhances the scaffold suitability for mineralization without the need for further surface modification, for example, plasma treatment, that may have an adverse effect on scaffold mechanical properties.

**Mechanical Properties.** Because the poly(PHB/PEG urethane)s are intended for scaffold application, they must have good mechanical properties not only in the dry state but also in the hydrated state. Pristine PHB is widely known as a brittle material because of its high crystallinity and occurrence of heterogeneous secondary crystallization.[38] Therefore, to reduce its brittleness, the two factors mentioned must be modulated. In this study, we couple soft PEG segments to hard PHB chains,

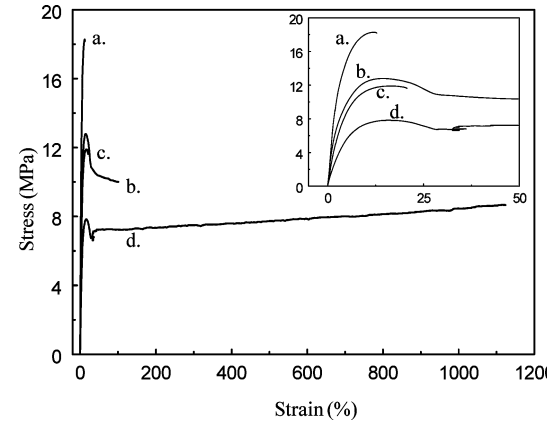


**Figure 7.** Stress−strain diagrams of poly(PHB/PEG urethane)s in dry state: (a) PH2E2(4:1), (b) PH1E2(5:1), (c) PH2E2(2:1), and (d) PH1E2(2.5:1).

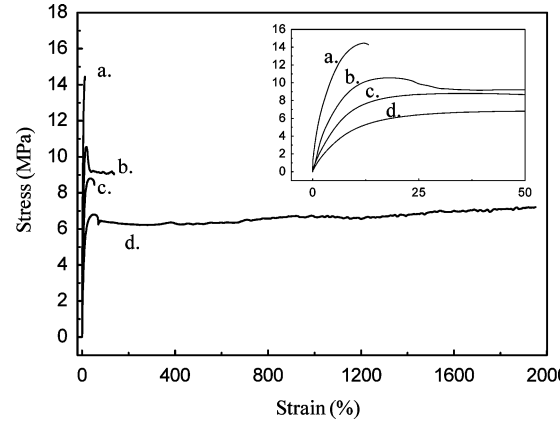


**Figure 8.** Stress−strain diagrams of poly(PHB/PEG urethane)s in hydrated state: (a) PH2E2(4:1), (b) PH1E2(5:1), (c) PH2E2(2:1), and (d) PH1E2(2.5:1).

with the aim of lowering PHB crystallinity and exploiting the plasticization effect of soft PEG. Moreover, with the use of short PHB-diols, a higher density of urethane bonds can be integrated into a single block copolymer chain. The stress−strain curve of the block copolymers in dry and hydrated states are plotted in Figures 7 and 8, respectively. Their dry and hydrated state tensile properties can be found in Table 3. The positive effect of adding PEG soft segments into the block copolymers is evident in all dry state data. All of the block copolymers have lower Young's modulus ($E$) and stress at break ($\sigma_b$) at 177 to 616 MPa and 9 to 18 MPa, respectively, as well as higher strain at break ($\varepsilon_b$) at 12 to 1090% as compared with those of pristine PHB, which are 1143 MPa, 26 MPa, and 2%, respectively.[20] The improvement in ductility can be attributed to the reduction of PHB crystallinity, the presence of urethane bonds, and the plasticization effect of soft PEG segment. The plasticization effect of PEG is better manifested in PH1E2(2.5:1) and PH1E2(5:1), where PHB segment length is shorter, with distinctive yielding process. As a result, with shorter PHB segment, highest PEG content, and low PHB crystallinity, PH1E2(2.5:1) shows the best improvement in ductility with 1090% strain before breaking. In comparison with our previous report[20] on poly(PHB/PEG urethane)s, this level of improvement could only be attained with 70% or more PEG content. But here, with the use of short PHB segment, we can achieve this at 50% PEG content as the result of relatively lower PHB crystallinity and higher urethane bond density along the block copolymer backbone.

**TABLE 3: Mechanical Properties of Poly(PHB/PEG urethane)s in Dry State and Hydrated State**

| poly(PHB/PEG urethane)[a] | | $E$ (MPa)[b] | $\sigma_y$ (MPa)[b] | $\varepsilon_y$ (%)[b] | $\sigma_b$ (MPa)[b] | $\varepsilon_b$ (%)[b] |
|---|---|---|---|---|---|---|
| PH1E2(2.5:1) | D state[c] | 177.7 ± 14.0 | 7.9 ± 0.4 | 19 ± 2 | 9.1 ± 0.3 | 1090 ± 25 |
| | H state[d] | 90.7 ± 6.6 | 6.3 ± 0.4 | 43 ± 9 | 6.8 ± 0.4 | 1962 ± 159 |
| PH1E2(5:1) | D state | 428.8 ± 19.1 | 12.8 ± 1.8 | 14 ± 1 | 11.3 ± 0.5 | 100 ± 7 |
| | H state | 277.7 ± 61.4 | 10.5 ± 0.7 | 20 ± 1 | 9.1 ± 1.5 | 135 ± 12 |
| PH2E2(2:1) | D state | 284.9 ± 35.4 | | | 11.1 ± 1.2 | 20 ± 1 |
| | H state | 136.5 ± 9.7 | | | 8.7 ± 0.2 | 57 ± 3 |
| PH2E2(4:1) | D state | 616.4 ± 77.9 | | | 18.0 ± 1.7 | 12 ± 1 |
| | H state | 342.7 ± 75.4 | | | 14.5 ± 1.3 | 13 ± 1 |

[a] Poly(PHB/PEG urethane)s are denoted PH$p$E$q$($a$:$b$), where $p$ and $q$ represent the indicative molecular weight of PHB-diol and PEG in kilograms per mole, respectively, whereas $a$:$b$ depicts the molar feed ratio of PHB-diol to PEG. [b] Mechanical properties were assessed by using Instron 5543 at a deformation rate of 40 mm·$\mu$min$^{-1}$; $E$: Young's modulus; $\sigma_y$: stress at yield; $\varepsilon_y$: strain at yield; $\sigma_b$: stress at break; $\varepsilon_b$: strain at break. [c] Dry state. [d] Hydrated state.

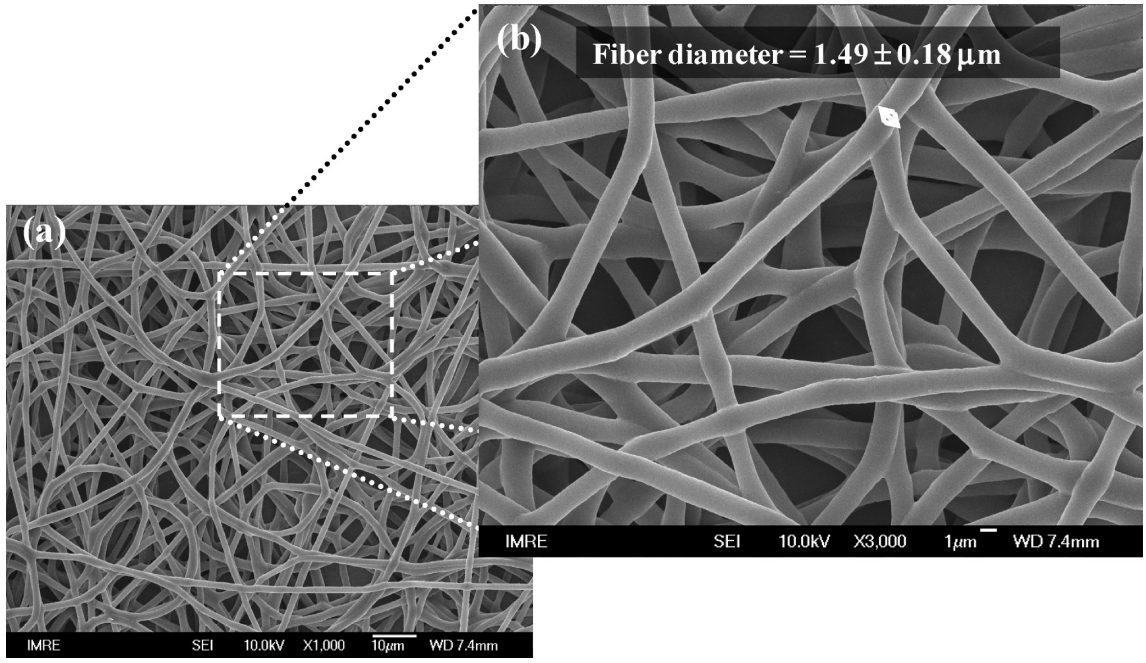


**Figure 9.** SEM images of electrospun fibers from PH2E2(4:1) under different magnifications. Scale bar in (a) and (b) corresponds to length scale of 10 and 1 $\mu$m, respectively.

In the hydrated state, all of the block copolymers have lower $E$ and $\sigma_b$ as well as higher $\varepsilon_b$ than those in the dry state. For PH1E2(2.5:1) and PH1E2(5:1), their yielding processes also occur at lower stress ($\sigma_y$) and higher strain ($\varepsilon_y$). The changes can be explained by the toughening effect brought about by absorbed water molecules.[39] When the block copolymers are immersed in water, water molecules are quickly absorbed into the polymer matrix with the aid from built-in PEG segments. As some PEG segments are also trapped within PHB crystalline lamellae, water molecules can now diffuse into the otherwise inaccessible region. Under external stress, the absorbed water molecules function as lubricant, facilitating the sliding over of PHB lamellae with one another and hence leading to lower $E$ and $\sigma_b$ and higher $\varepsilon_b$. In the case of PH1E2(2.5:1), the strain at break almost doubles to 1962%, whereas that of PH2E2(2:1) almost triples from 20 to 57%. Meanwhile, block copolymers that are of lesser PEG content: PH1E2(5:1) and PH2E2(4:1), experience smaller improvements. The capping of PEG content below 50 wt % in the present study serves to safeguard the mechanical integrity of the block copolymers from failures arising from excessive water swelling.[39]

**Electrospun Fibers and Their Calcium Mineralization.** The SEM pictures of electrospun PH2E2(4:1) are shown in Figure 9. It can be seen that the obtained fibers have uniformly smooth morphology with average diameter of 1.49 ± 0.18 $\mu$m. Collectively, the randomly oriented fibers form a 3D fibrous network with interconnected voids of micrometer sizes. To customize the fibers' surface chemistry for bone regeneration application, the electrospun fibers were immersed in SBF to facilitate calcium phosphate mineralization. After 12 h of immersion in ×10 SBF, PH2E2(4:1) scaffold is fully covered with calcium phosphate that gives rise to a very rough surface (Figure 10-Ic). When the top few layers of the scaffold were peeled away, extensive mineralization could still be seen within the scaffold construct (Figure 10-Id). This is in contrast with PHBV scaffold, which only has mineralization predominantly on the top few layers (Figure 10-Ia,b). To retain the porous architecture of mineralized PH2E2(4:1) scaffold, another round of coating in a more dilute ×2.5 SBF was carried out over the same period of time. As shown in Figure 10-Ie, mineralization on the scaffold is now very controlled with the fibrous network morphology well preserved. Again, when the first few layers were peeled away, we could still find the inner layers of the PH2E2(4:1) scaffold evenly mineralized. The amount of minerals formed on the fiber mats were quantified using TGA where samples were heated up to 800 °C under $N_2$ atmosphere. At this temperature, the polymeric fibers were completely degraded and the amount of residue left behind should correspond to

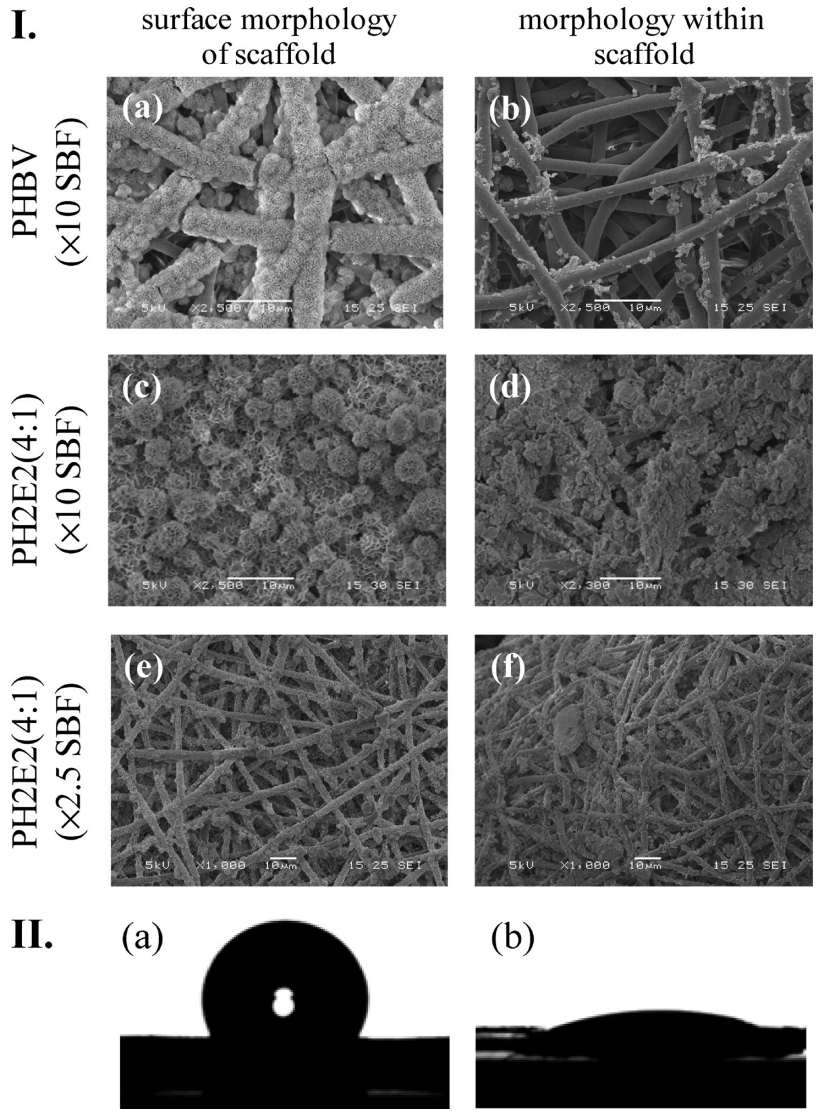


**Figure 10.** (I) SEM pictures of scaffolds after 12 h immersion in ×10 or ×2.5 simulated body fluid (SBF). Scale bar in the images corresponds to a length scale of 10 $\mu$m. (II) Photographs of water droplet on electrospun scaffold of (a) PHBV and (b) PH2E2(4:1).

minerals content. It was found that the residues left from the PH2E2(4:1) fiber mats that were previously immersed in ×10 and ×2.5 SBF amounted to 42 and 17 wt %, respectively. In a separate TGA analysis, we also found that the pure minerals left 78 wt % of residue when heated to 800 °C. Thus, after correcting for the weight loss due to minerals, the minerals content of the mineralized PH2E2(4:1) fiber mats in ×10 and ×2.5 SBF are around 54 and 22 wt %, respectively. In contrast, the mineralized PHBV fiber mat that was immersed in ×10 SBF contains only 10 wt % of minerals. The much more superior mineralization in our PH2E2(4:1) scaffold over PHBV can be attributed to its hydrophilic nature. Electrospun scaffolds of hydrophobic polyesters usually give higher static water contact angle as compared with their flat films because of greater surface roughness. For PHBV, its water contact angle increases from 82° for spin-coated thin film to 123° for electrospun fibrous mat (Figure 10-IIa). As a result, this aggravates wetting problem on the electrospun fibrous scaffold and limits mineralization. The situation is reversed for PH2E2(4:1). Its electrospun fibrous mat shows a static water contact angle of 23° (Figure 10-IIb), much lower than its spin-coated thin film at 74°. The apparently lower water contact angle is due to seeping in of water into the porous scaffold as a result of its hydrophilic nature. This in turn proves advantageous for mineralization as it allows access of SBF deep into the inner layers of scaffold. In addition to the improved wetting characteristics, the PEG segments present in the poly(PHB/PEG urethane) also aid in the nucleation and growth of calcium minerals.

In the mineralization of most electrospun hydrophobic polyester scaffold, surface modifications are usually required to improve hydrophilicity prior to actual mineralization.[35] The process typically involves plasma treatment or alkaline treatment, which impart hydrophilicity through creation of charged species on substrate surface via breaking of covalent bonds. In view of the micrometer to submicrometer dimension of electrospun fibers, the treatment may lead to substantial loss in mechanical properties on resultant scaffold. With the use of poly(PHB/PEG urethane), plasma or alkaline treatment are no longer necessary as some degree of hydrophilicity is built into the block copolymer. This not only simplifies the mineralization process, it also avoids the potential harmful effect of the surface treatment on scaffold materials. Essentially, due to its improved hydrophilicity, the electrospun poly(PHB/PEG urethane) scaffold can be easily mineralized by a simple incubation in appropriate solution, even deep into the scaffold construct. This is important for fabrication of mineralized 3D scaffolds.

## Conclusions

Through rational design, a series of poly(PHB/PEG urethane) block copolymers with good mechanical properties has been successfully synthesized. The use of short PHB segment in the block copolymerization has allowed us to synthesize poly(PHB/PEG urethane)s with low PHB crystallinity and hence better ductility with incorporation of only 50 wt % or less of PEG. The low PEG content in the block copolymer ensured dimensional stability of the electrospun fibrous polymer scaffold immersed in body fluid. Moreover, with the optimum PEG content built-in, the block copolymers demonstrated enhanced ductility in hydrated state by capitalizing on the lubricating effect of water absorbed.

When electrospun into fibrous scaffold, the poly(PHB/PEG urethane) scaffold outperformed its PHBV counterpart by demonstrating improved wettability and nice coating with calcium minerals throughout the scaffold construct by simple incubation in SBF, without further surface treatment. With a customized surface chemistry, the scaffold may be useful for bone regeneration applications and can possibly be extended to other types of tissue by coating other biologically significant compounds.

**Acknowledgment.** We acknowledge the financial support from Agency for Science, Technology and Research (A*STAR) of Singapore and National University of Singapore (NUS). We thank Prof. Kam W. Leong of Department of Biomedical Engineering, Duke University for his valuable suggestions and helpful discussions.

**Supporting Information Available:** Representative thermal degradation profile of PH2E2(4:1), DSC first cooling curves, water uptake profiles of the poly(PHB/PEG urethane)s, and SEM image of PH2E2(4:1) fibrous scaffold with fibroblast cells proliferated on it after 4 days of incubation. This material is available free of charge via the Internet at http://pubs.acs.org.

## References and Notes

(1) Langer, R.; Vacanti, J. P. *Science* **1993**, *260*, 920–926.
(2) Khademhosseini, A.; Langer, R.; Borenstein, J.; Vacanti, J. P. *Proc. Natl. Acad. Sci. U.S.A.* **2006**, *103*, 2480–2487.
(3) Mohammed, J. S.; Murphy, W. L. *Adv. Mater.* **2009**, *21*, 2361–2374.
(4) Place, E. S.; Evans, N. D.; Stevens, M. M. *Nat. Mater.* **2009**, *8*, 457–470.
(5) Fernandes, H.; Moroni, L.; van Blitterswijk, C.; de Boer, J. *J. Mater. Chem.* **2009**, *19*, 5474–5484.
(6) Karageorgiou, V.; Kaplan, D. *Biomaterials* **2005**, *26*, 5474–5491.
(7) Ma, P. X. *Adv. Drug Delivery Rev.* **2008**, *60*, 184–198.
(8) Liang, D.; Hsiao, B. S.; Chu, B. *Adv. Drug Delivery Rev.* **2007**, *59*, 1392–1412.
(9) Barnes, C. P.; Sell, S. A.; Boland, E. D.; Simpson, D. G.; Bowlin, G. L. *Adv. Drug Delivery Rev.* **2007**, *59*, 1413–1433.
(10) Pompe, T.; Keller, K.; Mothes, G.; Nitschke, M.; Teese, M.; Zimmermann, R.; Werner, C. *Biomaterials* **2007**, *28*, 28–37.
(11) Zhao, K.; Deng, Y.; Chen, G. Q. *Biochem. Eng. J.* **2003**, *16*, 115–123.
(12) Zheng, Z.; Bei, F. F.; Tian, H. L.; Chen, G. Q. *Biomaterials* **2005**, *26*, 3537–3548.
(13) Doi, Y. *Microbial Polyester*; VCH Publisher: New York, 1990.
(14) Avella, M.; Martuscelli, E. *Polymer* **1988**, *29*, 1731–1737.
(15) Verhoogt, H.; Ramsay, B. A.; Favis, B. D. *Polymer* **1994**, *35*, 5155–5169.
(16) Kumagai, Y.; Kanesawa, Y.; Doi, Y. *Makromol. Chem.* **1992**, *193*, 53–57.
(17) Chen, G. Q.; Zhang, G.; Park, S. J.; Lee, S. Y. *Appl. Microbiol. Biotechnol.* **2001**, *57*, 50–55.
(18) Chen, G. Q.; Wu, Q. *Biomaterials* **2005**, *26*, 6565–6578.
(19) Doi, Y. *Macromol. Symp.* **1995**, *98*, 585–599.
(20) Li, X.; Loh, X. J.; Wang, K.; He, C. B.; Li, J. *Biomacromolecules* **2005**, *6*, 2740–2747.
(21) Li, X.; Liu, K. L.; Li, J.; Tan, E. P. S.; Chan, L. M.; Lim, C. T.; Goh, S. H. *Biomacromolecules* **2006**, *7*, 3112–3119.
(22) Saad, G. R.; Lee, Y. J.; Seliger, H. *J. Appl. Polym. Sci.* **2002**, *83*, 703–718.
(23) Saad, G. R.; Seliger, H. *Polym. Degrad. Stab.* **2004**, *83*, 101–110.
(24) Andrade, A. P.; Neuenschwander, P.; Hany, R.; Egli, T.; Witholt, B.; Li, Z. *Macromolecules* **2002**, *35*, 4946–4950.
(25) Zhang, X. Q.; Yang, H.; Liu, Q. W.; Zheng, Y.; Xie, H. F.; Wang, Z. L.; Cheng, R. S. *J. Polym. Sci., Part A: Polym. Chem.* **2005**, *43*, 4857–4869.
(26) Reeve, M. S.; McCarthy, S. P.; Gross, R. A. *Macromolecules* **1993**, *26*, 888–894.
(27) Ravenelle, F.; Marchessault, R. H. *Biomacromolecules* **2002**, *3*, 1057–1064.
(28) Li, J.; Li, X.; Ni, X. P.; Leong, K. W. *Macromolecules* **2003**, *36*, 2661–2667.
(29) Chen, Z.; Cheng, S.; Li, Z.; Xu, K.; Chen, G.-Q. *J Biomater. Sci., Polym. Ed.* **2009**, *20*, 1451–1471.
(30) Chen, Z. F.; Cheng, S. T.; Xu, K. T. *Biomaterials* **2009**, *30*, 2219–2230.
(31) Pan, J. Y.; Li, G. Y.; Chen, Z. F.; Chen, X. Y.; Zhu, W. F.; Xu, K. T. *Biomaterials* **2009**, *30*, 2975–2984.
(32) Loh, X. J.; Zhang, Z. X.; Wu, Y. L.; Lee, T. S.; Li, J. *Macromolecules* **2009**, *42*, 194–202.
(33) Li, X.; Liu, K. L.; Wang, M.; Wong, S. Y.; Tjiu, W. C.; He, C. B.; Goh, S. H.; Li, J. *Acta Biomater.* **2009**, *5*, 2002–2012.
(34) Hirt, T. D.; Neuenschwander, P.; Suter, U. W. *Macromol. Chem. Phys.* **1996**, *197*, 1609–1614.
(35) Yang, F.; Wolke, J. G. C.; Jansen, J. A. *Chem. Eng. J.* **2008**, *137*, 154–161.
(36) Gunaratne, L.; Shanks, R. A.; Amarasinghe, G. *Thermochim. Acta* **2004**, *423*, 127–135.
(37) Wang, C.; Hsu, C.-H.; Hwang, I. H. *Polymer* **2008**, *49*, 4188–4195.
(38) Barham, P. J.; Keller, A. *J. Polym. Sci., Part B: Polym. Phys.* **1986**, *24*, 69–77.
(39) Xu, J.; Bohnsack, D. A.; Mackay, M. E.; Wooley, K. L. *J. Am. Chem. Soc.* **2007**, *129*, 506–507.

JP1018247